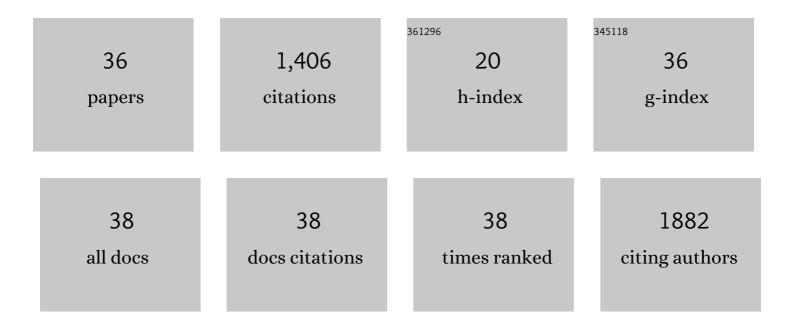
Benjamin M Tutolo

List of Publications by Year in descending order

Source: https://exaly.com/author-pdf/3855066/publications.pdf Version: 2024-02-01



#	Article	IF	CITATIONS
1	Expanding the role of reactive transport models in critical zone processes. Earth-Science Reviews, 2017, 165, 280-301.	4.0	207
2	The Lost City hydrothermal system: Constraints imposed by vent fluid chemistry and reaction path models on subseafloor heat and mass transfer processes. Geochimica Et Cosmochimica Acta, 2015, 163, 59-79.	1.6	104
3	Decrease in CO2 efflux from northern hardwater lakes with increasing atmospheric warming. Nature, 2015, 519, 215-218.	13.7	102
4	Experimental dissolution of dolomite by CO2-charged brine at 100°C and 150bar: Evolution of porosity, permeability, and reactive surface area. Chemical Geology, 2014, 380, 145-160.	1.4	94
5	CO2 sequestration in feldspar-rich sandstone: Coupled evolution of fluid chemistry, mineral reaction rates, and hydrogeochemical properties. Geochimica Et Cosmochimica Acta, 2015, 160, 132-154.	1.6	87
6	Hydrothermal Transport of Ag, Au, Cu, Pb, Te, Zn, and Other Metals and Metalloids in New Zealand Geothermal Systems: Spatial Patterns, Fluid-Mineral Equilibria, and Implications for Epithermal Mineralization. Economic Geology, 2016, 111, 589-618.	1.8	70
7	Nanoscale constraints on porosity generation and fluid flow during serpentinization. Geology, 2016, 44, 103-106.	2.0	68
8	Magnetite authigenesis and the warming of early Mars. Nature Geoscience, 2018, 11, 635-639.	5.4	66
9	Permeability, porosity, and mineral surface area changes in basalt cores induced by reactive transport of <scp>CO</scp> ₂ â€rich brine. Water Resources Research, 2017, 53, 1908-1927.	1.7	65
10	Experimental examination of the Mg-silicate-carbonate system at ambient temperature: Implications for alkaline chemical sedimentation and lacustrine carbonate formation. Geochimica Et Cosmochimica Acta, 2018, 225, 80-101.	1.6	56
11	DBCreate: A SUPCRT92-based program for producing EQ3/6, TOUGHREACT, and GWB thermodynamic databases at user-defined T and P. Computers and Geosciences, 2013, 51, 415-417.	2.0	53
12	Whole rock basalt alteration from CO2-rich brine during flow-through experiments at 150 ŰC and 150 bar. Chemical Geology, 2017, 453, 92-110.	1.4	52
13	High performance reactive transport simulations examining the effects of thermal, hydraulic, and chemical (THC) gradients on fluid injectivity at carbonate CCUS reservoir scales. International Journal of Greenhouse Gas Control, 2015, 39, 285-301.	2.3	39
14	Serpentinization as a reactive transport process: The brucite silicification reaction. Earth and Planetary Science Letters, 2018, 484, 385-395.	1.8	34
15	Internal consistency in aqueous geochemical data revisited: Applications to the aluminum system. Geochimica Et Cosmochimica Acta, 2014, 133, 216-234.	1.6	33
16	Permeability Reduction Produced by Grain Reorganization and Accumulation of Exsolved CO ₂ during Geologic Carbon Sequestration: A New CO ₂ Trapping Mechanism. Environmental Science & Technology, 2013, 47, 242-251.	4.6	32
17	Serpentinization of olivine at 300 °C and 500 bars: An experimental study examining the role of silica on the reaction path and oxidation state of iron. Chemical Geology, 2017, 475, 122-134.	1.4	29
18	A seawater throttle on H ₂ production in Precambrian serpentinizing systems. Proceedings of the National Academy of Sciences of the United States of America, 2020, 117, 14756-14763.	3.3	28

Benjamin M Tutolo

#	Article	IF	CITATIONS
19	Serpentine–Hisingerite Solid Solution in Altered Ferroan Peridotite and Olivine Gabbro. Minerals (Basel, Switzerland), 2019, 9, 47.	0.8	22
20	Experimental Observation of Permeability Changes In Dolomite at CO ₂ Sequestration Conditions. Environmental Science & amp; Technology, 2014, 48, 140203132426009.	4.6	21
21	Alkalinity Generation Constraints on Basalt Carbonation for Carbon Dioxide Removal at the Gigaton-per-Year Scale. Environmental Science & amp; Technology, 2021, 55, 11906-11915.	4.6	21
22	Chemical and physical changes during seawater flow through intact dunite cores: An experimental study at 150–200 °C. Geochimica Et Cosmochimica Acta, 2017, 214, 86-114.	1.6	17
23	Anhydrite solubility in low-density hydrothermal fluids: Experimental measurements and thermodynamic calculations. Chemical Geology, 2019, 524, 184-195.	1.4	17
24	A Series of Data-Driven Hypotheses for Inferring Biogeochemical Conditions in Alkaline Lakes and Their Deposits Based on the Behavior of Mg and SiO2. Minerals (Basel, Switzerland), 2021, 11, 106.	0.8	14
25	PyGeochemCalc: A Python package for geochemical thermodynamic calculations from ambient to deep Earth conditions. Chemical Geology, 2022, 606, 120984.	1.4	13
26	Implications of the redissociation phenomenon for mineral-buffered fluids and aqueous species transport at elevated temperatures and pressures. Applied Geochemistry, 2015, 55, 119-127.	1.4	9
27	Geochemical evaluation of glauconite carbonation during sedimentary diagenesis. Geochimica Et Cosmochimica Acta, 2021, 306, 226-244.	1.6	8
28	Magmatic carbon outgassing and uptake of CO2 by alkaline waters. American Mineralogist, 2020, 105, 28-34.	0.9	7
29	Experimental evaluation of the role of redox during glauconite-CO2-brine interactions. Applied Geochemistry, 2020, 115, 104558.	1.4	7
30	Alternate routes to sustainable energy recovery from fossil fuels reservoirs. Part 1. Investigation of high-temperature reactions between sulfur oxy anions and crude oil. Fuel, 2021, 302, 121050.	3.4	7
31	A rate law for sepiolite growth at ambient temperatures and its implications for early lacustrine diagenesis. Geochimica Et Cosmochimica Acta, 2020, 288, 301-315.	1.6	6
32	Probing the application of kinetic theory to Mg-phyllosilicate growth with Si isotope doping. Geochimica Et Cosmochimica Acta, 2021, 310, 205-220.	1.6	5
33	Evaluation of the potential of glauconite in the Western Canadian Sedimentary Basin for large-scale carbon dioxide mineralization. International Journal of Greenhouse Gas Control, 2022, 117, 103663.	2.3	5
34	Experimental partitioning of osmium between pyrite and fluid: Constraints on the mid-ocean ridge hydrothermal flux of osmium to seawater. Geochimica Et Cosmochimica Acta, 2021, 293, 240-255.	1.6	4
35	Anhydrite replacement reaction in nodular pyrite breccia and its geochemical controls on the δ34S signature of pyrite in the TAG hydrothermal mound, 26° N Mid Atlantic Ridge. Lithos, 2021, 400-401, 106357.	0.6	2
36	Mineralogical characterization and thermodynamic modelling of scales formed in once through steam generators. Fuel, 2022, 308, 121990.	3.4	1